choices of rotation axes in Renninger scans to be used for phase determination have been given by Post, Nicolosi & Ladell (1984).

## APPENDIX I

### [Invariant triplet phases of diamond-type crystals

[In this Appendix we assume the validity of the 'conditions limiting possible reflections' as given in *International Tables for X-ray Crystallography* (1969), Vol. I, for positions 8($a$) in $Fd3m$.]

The structure factor may be written as $F(hkl) = 8f \cos 2\pi(h + k + l)/8$. Indices that sum to $4n + 2$ for individual reflections have structure factors whose magnitudes equal zero. Those are not considered here.

The indices of individual reflections are either all even or all odd. For the former, the sum of the indices equals $4n$; for the latter the sum is $4n \pm 1$. In either case, the phase of an individual reflection is positive if $n$ is even and negative if $n$ is odd.

We are concerned with invariant triplet phases; these are equal to the sums of the phases of three diffraction vectors which form triangles in reciprocal space. Invariance requires that all three reflections have even indices or that two have odd indices and the third even. The indices of the three reflections must sum to zero.

In the case of even-index reflections, all reflection phases as well as the corresponding triplet phase will be positive if all $n$'s are even. Since odd-index reflections must occur in pairs in invariant triplets, the third

reflection will have even indices. We write the relations among the three as:

$$4(n1) = [4(n2) \pm 1] + [4(n3) \pm 1].$$

In order that $n1$ be an integer, it is necessary that the $\pm 1$ terms cancel. This requires that one of the right-hand terms be of the type $4n + 1$ and the other of the type $4n - 1$. It follows that

$$4(n1) = 4(n2) + 4(n3),$$

a condition that is satisfied only if all the $n$'s are even or if two of the $n$'s are odd. For either of these cases the triplet phase will be positive.

#### References

BARTELS, W. J. (1983). *Philips Tech. Rev.* **41**, 183–185.
BUERGER, M. J. (1942). *X-ray Crystallography.* New York: John Wiley.
CHANG, S. L. (1982). *Acta Cryst.* **A38**, 516–521.
GONG, P. P. & POST, B. (1982). Am. Crystallogr. Assoc. Meet., Gaithersberg, Maryland. Abstract M6.
GONG, P. P. & POST, B. (1983). *Acta Cryst.* **A39**, 719–724.
HAN, F.-S. & CHANG, S. L. (1983). *Acta Cryst.* **A39**, 98–101.
HUMMER, K. & BILLY, H. (1984). Private communication.
*International Tables for X-ray Crystallography* (1969). Vol. I. Birmingham: Kynoch Press.
KEELING, R. O. (1957). *Acta Cryst.* **10**, 209–214.
LADELL, J. (1982). Am. Crystallogr. Assoc. Meet., Gaithersberg, Maryland. Abstract M8.
NICOLOSI, J. (1982). Am. Crystallogr. Assoc. Meet., Gaithersberg, Maryland. Abstract M7.
POST, B. (1983). *Acta Cryst.* **A39**, 711–718.
POST, B., NICOLOSI, J. & LADELL, J. (1984). *Acta Cryst.* **A40**, 684–688.

# The Effect of Measured *vs* Conventional Polarization Factors in Structure Refinements*

BY P. SUORTTI,† Å. KVICK AND T. J. EMGE‡

*Chemistry Department, Brookhaven National Laboratory, Upton, NY 11973, USA*

## Abstract

The polarization ratio $K$ is measured for LiF (200) and graphite (00.2) monochromators at different X-ray wavelengths. In each case the kinematical value $\cos^2 2\theta_M$ is a poor approximation, and the actual value of $K$ may exceed the dynamical limit $\cos 2\theta_M$. An explanation is offered in terms of a model that includes secondary extinction. The effects of an incorrect value of $K$ are studied by refining the model for a ruby standard crystal. The positional parameters are not affected, but the scale, extinction and thermal parameters change. The effects are, however, smaller than the ones observed in the structural parameters due to termination of the data set at lower $\sin \theta/\lambda$ values.

## I. Introduction

A good crystal monochromator for X-rays has large reflectivity within the angular range that contributes to the exit beam. The beam reflected from a flat crystal diverges, and the optimum width of the rocking curve is determined by the desired size of the beam at the sample crystal, and the reflecting range of a focusing crystal should match the width of the source. In practice the choice is limited to a few materials that can meet the technical requirements, and the typical rocking-curve widths vary from 0.3° (graphite) to a few seconds of arc (quartz, Ge, Si). The peak reflectivities vary from a few tens of percent to almost total reflection.

The monochromator changes the degree of polarization of the X-ray beam, and customarily these changes are calculated by applying kinematical diffraction theory to the monochromator crystal. However, it is easy to demonstrate that a good monochromator is very far from the kinematical limit. The integrated reflectivity per unit length, $Q$, is defined by (James, 1962, pp. 50–51)

$$Q\bar{t} = \int R(\varphi) \, d\varphi = R(0) \, \Delta\varphi, \qquad (1)$$

where $R(\varphi)$ is the reflectivity as a function of the rocking angle $\varphi = \theta - \theta_B$ and where $\Delta\varphi$ is the integral width of the reflection. In the symmetrical Bragg case the effective thickness is $\bar{t} = 1/2\mu$, where $\mu$ is the total attenuation coefficient. If we consider secondary extinction only and assume a Gaussian rocking curve of variance $\eta$ (Zachariasen, 1945, pp. 164–168),

$$Q/2\mu = 1 + \mu_0/gQ - [(1 + \mu_0/gQ)^2 - 1]^{1/2}, \quad (2)$$

where $g = (2\pi^{1/2}\eta)^{-1}$, and $\mu_0$ is the attenuation coefficient due to photoelectric effect and inelastic scattering. In the second-order approximation $\mu = \mu_0 + gQ$.

The value of $Q$ is obtained from kinematical theory;

$$Q = r_e^2(\lambda^3 K_{pol}/\sin 2\theta)(F^2/V_c^2), \qquad (3)$$

where $r_e = e^2/mc^2$ is the classical electron radius, $\lambda$ the X-ray wavelength and $F$ the structure factor of a unit cell with volume $V_c$. The polarization factor is 1 for the $\sigma$ component perpendicular to the plane of diffraction and $\cos^2 2\theta$ for the $\pi$ component in that plane. The integrated polarization ratio of the monochromator is defined as

$$K = \int R_\pi(\varphi) \, d\varphi / \int R_\sigma(\varphi) \, d\varphi \leq 1. \qquad (4)$$

For a concrete example, consider graphite (00.2) monochromator with $\eta = 0.125°$ ($g = 130$) and calculate $K$ at $\lambda = 1\cdot542$ Å. The kinematical reflectivities are $Q_\sigma = 0\cdot152$ cm$^{-1}$ and $Q_\pi = 0\cdot122$ cm$^{-1}$, $\mu_0 = 9\cdot5$ cm$^{-1}$, and with these values $K = 0\cdot904$, while $\cos 2\theta_M = 0\cdot894$ and $\cos^2 2\theta_M = 0\cdot800$.

The above calculation is far too simplified to give a reliable estimate for the polarization ratio $K$, but it demonstrates that the kinematical value of $K$ is certainly a poor estimate and that the actual value may exceed the dynamical limit. This is well documented and discussed by many authors (for references, see Jennings, 1984). The purpose of the present note is to describe a simple method for the experimental determination of $K$, give some results, and discuss the possible implications in single-crystal structure refinement in the light of a representative example.

## II. Measurement of polarization

The beam of characteristic radiation as transmitted by the crystal monochromator can be considered to consist of two independent components, denoted by $\sigma$ and $\pi$ (Fig. 1). The components can be separated by two methods: anomalous transmission in a thick perfect crystal or 90° reflection. The latter is based on the fact that the elastic and Compton scattering amplitudes are proportional to $(\mathbf{e}_1 . \mathbf{e}_2)$, where $\mathbf{e}_1$ and $\mathbf{e}_2$ are polarization vectors of the incident and scattered beams, respectively. The background from multiple and resonant scattering has different polarization dependence, and the determination of the $\pi$ to $\sigma$ ratio must be based on Bragg scattering, which is separated from this background. The details of this aspect are discussed elsewhere (Materlik & Suortti, 1984).

90° reflection from a powder sample was used in the present work. This technique has several advantages. The intensity is proportional to $(\mathbf{e}_1 . \mathbf{e}_2)^2$, which enhances the separation and allows a few degrees deviation from the condition that $2\theta = 90°$; in the present measurements the contribution of the $\pi$ component was less than 0·2%. This makes it possible to cover most wavelengths using different reflections from one powder sample. No angular scan is needed, if the receiving slit is wide enough to encompass the reflection. However, spinning the sample about the surface normal is essential to average the effects of inhomogeneities and preferred orientation. The polarizer is essentially a simple powder diffractometer that can be rotated about the incident beam in order
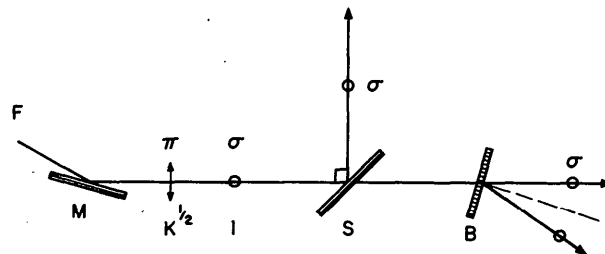


Fig. 1. Polarization of the monochromated X-ray beam; the $\sigma$ component has the electric vector perpendicular to the plane of diffraction at the monochromator $M$, $\pi$ component parallel to this plane. The ratio of the amplitudes is $1 : K^{1/2}$. The components can be separated by a 90° reflection at the sample $S$ or by anomalous transmission through the Borrmann crystal $B$.

Table 1. *Polarization ratios for* LiF(200) *and graphite* (00.2) *monochromators*

The experimental values $K_{exp}$ were determined using reflections from an Mo powder sample, and the values $K_{calc}$ were calculated from (2). Characteristic radiations from Mo, Cu and Co X-ray tubes are used.

| | $\lambda$ | $\cos 2\theta_M$ | $\cos^2 2\theta_M$ | $hkl$ | $2\theta$ | $K_{exp}$ | $g$ | $K_{calc}$ |
|---|---|---|---|---|---|---|---|---|
| LiF(200) | 0·7107 | 0·938 | 0·879 | 611 | 88·23 | 0·93(1) | 325 | 0·939 |
| | 1·7902 | 0·605 | 0·366 | 211 | 88·33 | 0·60(2) | | 0·671 |
| Graphite(00.2) | 1·5418 | 0·894 | 0·800 | 220 | 87·72 | 0·91(1) | 130 | 0·904 |

to vary the plane of diffraction between horizontal and vertical. The position of the receiving slit can be changed by a few degrees on both sides of $2\theta = 90°$ by a linear drive, which is coupled to a potentiometer that is used to indicate the position. The actual construction is described elsewhere (Materlik & Suortti, 1984), and it is designed to maintain the geometrical conditions unchanged when the polarizer is rotated. However, minor changes of the incident intensity are possible if the collimators are not perfectly centered, and the intensities were in our case normalized by measuring fluorescence from a plate inserted in front of the powder sample or by a direct measurement of the primary beam intensity.

Reflections from an Mo powder sample were used in the present measurement. The monochromators were a plastically bent LiF(200) and a flat graphite (00.2). Characteristic Mo $K\alpha$, Cu $K\alpha$ and Co $K\alpha$ radiation was assumed to be unpolarized. The details and results of the measurement are collected in Table 1. The values for LiF are close to $\cos 2\theta_M$, as in the case of dynamical diffraction. This monochromator is made by bending and gluing a thin crystal plate, which is heated to 373 K, on a curved mount, and this results in fracturing to mosaic blocks that are large enough to exhibit primary extinction. Nevertheless, (2), which accounts for secondary extinction only, overestimates the polarization ratio only slightly. In the case of graphite the theoretical 'guess' is very close to the experimental value. The present findings are in line with earlier observations, although individual LiF crystals seem to vary much more than the pyrolytic graphite crystals used as monochromators (Suortti & Jennings, 1977; Le Page, Gabe & Calvert, 1979).

Some measurements indicate that $K$ is not uniquely defined for a given crystal, but depends on the monochromator geometry as well. This is discussed by Jennings (1981) and Olekhnovich, Markovich, Olekhnovich & Poluchankina (1981). The point is what range of the reflectivity curve $R(\varphi)$ of the monochromator contributes to the beam used in the measurement and, therefore, $K$ should always be measured for the beam that actually hits the sample.

### III. Polarization factor in structure refinement

If the sample crystal can be assumed to diffract kinematically, the integrated count of a reflection

scanned at angular velocity $\omega$ is

$$n_{hkl} = (n_0/\omega)AQ\bar{\imath} \sim (K_{pol}/C)F_o^2, \qquad (5)$$

where $n_0$ is the incident flux, $C$ the scale and $A$ is the absorption factor. The polarization factor can be written as follows:

$$K_{pol} = (1 + \alpha \cos^2 2\theta)/(1 + \alpha), \qquad (6)$$

where $\alpha = K$ when the plane of diffraction at the monochromator is parallel to that at the sample, and $\alpha = 1/K$ when the planes are perpendicular. The intermediate cases have been worked out by Olekhnovich (1969).

An incorrect value of $\alpha$ causes an error in $F_o^2$, which is zero at $2\theta = 0$ and 180° and maximum at $2\theta = 90°$. Fig. 2 shows the correction that must be applied to $F_o^2$'s when the kinematical value $\alpha = 1/\cos^2 2\theta_M = 1·25$ is replaced by the measured value $\alpha = 1/0·91 = 1·10$ for graphite (00.2) with Cu $K\alpha$ radiation. Conversely, if the incorrect value of $\alpha$ is used, this function is accommodated by changes in the parameters of the model. Fig. 2 shows schematically how $F_c^2$'s are affected by changes of the average thermal parameter, extinction correction and scale factor.
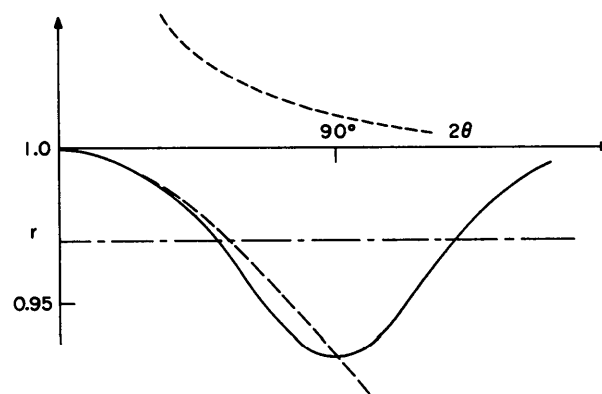


Fig. 2. Effects of various factors on $F_o^2$ (observed) and $F_c^2$ (calculated). $F_o^2$ is to be multiplied by the function given by the solid line, when the assumed value $\alpha = 1·25$ is replaced by the measured value $\alpha = 1·10$; these apply to a graphite (00.2) monochromator with Cu $K\alpha$ radiation. This function can be accommodated by the scale factor, Debye-Waller factor, and extinction correction of the model. The lower dashed line indicates the effect on $F_c^2$ of increasing the average thermal parameter of the model by $\Delta B = 0·165$ Å$^2$, the dot-dashed line lowering the scale by 3%, and upper dotted line the additional effect of a change in the average extinction correction.

Table 2. *Model parameters for ruby standard cyrstal when* $\alpha = 1\cdot10$ *and* $1\cdot25$

The data set is terminated at maximum scattering angle $2\theta_{max}$. $C$ is the scale factor and $B$ is the average of the thermal parameters of Al and O, $B = 8\pi^2 \frac{1}{6} \sum U_{ii}$, where the $U_{ii}$'s are listed in Table 3. $\Gamma$ is the extinction parameter. $R$ is the conventional agreement factor, and $S = [\sum w|F_o^2 - F_c^2|^2/(N-P)]^{1/2}$, where $N$ is the number of reflections used and $P$ is the number of variables refined.

|  | sin θ/λ <0·63 Å⁻¹ | | sin θ/λ <0·55 Å⁻¹ | | sin θ/λ <0·5 Å⁻¹ | |
| --- | --- | --- | --- | --- | --- | --- |
| $2\theta_{max}$ | 150° | 150° | 116° | 116° | 100° | 100° |
|  | (a) | (b) | (c) | (d) | (e) | (f) |
| $\alpha$ | 1·10 | 1·25 | 1·10 | 1·25 | 1·10 | 1·25 |
| $C$ | 0·0247 (3) | 0·0242 (3) | 0·0240 (3) | 0·0236 (3) | 0·0228 (3) | 0·0229 (3) |
| $\Delta d(\%)$ |  | −1·7 |  | −1·7 |  | 0·0 |
| $\frac{1}{6}\sum U_{ii}$ (Å²) | 0·0131 (3) | 0·0136 (3) | 0·0166 (5) | 0·0163 (5) | 0·0242 (11) | 0·0217 (11) |
| $\Delta B$(Å²) |  | 0·04 (3) |  | −0·02 (6) |  | −0·2 (1) |
| $\Gamma$‡ | 33 (5) | 28 (5) | 29 (8) | 32 (7) | 29* | 29* |
| $R$ | 0·039 | 0·037 | 0·043 | 0·075 | 0·051 | 0·035 |
| $S$ | 2·14 | 2·12 | 2·13 | 2·09 | 2·32 | 1·70 |
| $N$ | 350† | 372† | 246 | 246 | 165 | 151 |

* Value constrained in the refinement.

† Reflections with extinction >1·2 were omitted from the refinements thus producing different numbers of included reflections. All parameters shifted less than 0·6σ if the extinction cut-off limits were set to produce equal numbers of included reflections.

‡ ×10⁻².

Table 3. *Positional* $(\times 10^5)$ *and thermal parameters* $(Å^2 \times 10^4)$

The thermal factor is $\exp[-2\pi^2(U_{11}h^2a^{*2}\cdots+2U_{12}^*hk^*a^*b^*\cdots)]$. The different lines (a)-(f) refer to refinements described in Table 2.

|  |  | $x$ | $y$ | $z$ | $U_{11}=U_{22}$ | $U_{33}$ | $U_{12}$ | $U_{13}$ |
| --- | --- | --- | --- | --- | --- | --- | --- | --- |
| Al | (a) | 0 | 0 | 35 215 (3) | 118 (5) | 106 (9) | 0 | 0 |
|  | (b) |  |  | 35 217 (3) | 116 (5) | 120 (9) |  |  |
|  | (c) |  |  | 35 224 (6) | 135 (7) | 157 (15) |  |  |
|  | (d) |  |  | 35 228 (6) | 130 (7) | 152 (15) |  |  |
|  | (e) |  |  | 35 277 (18) | 147 (15) | 324 (42) |  |  |
|  | (f) |  |  | 35 276 (17) | 129 (13) | 299 (38) |  |  |
| O | (a) | 69 323 (20) | 0 | 25 000 | 156 (6) | 134 (7) | 73 (5) | 43 (9) |
|  | (b) | 69 349 (19) |  |  | 161 (6) | 140 (7) | 80 (5) | 34 (9) |
|  | (c) | 69 371 (29) |  |  | 189 (11) | 189 (16) | 88 (8) | 123 (9) |
|  | (d) | 69 391 (28) |  |  | 188 (11) | 189 (16) | 89 (8) | 121 (10) |
|  | (e) | 69 450 (27) |  |  | 236 (19) | 362 (36) | 118 (14) | 63 (24) |
|  | (f) | 69 434 (25) |  |  | 214 (16) | 316 (35) | 108 (12) | 64 (21) |

As an example of an actual situation the model for the diffraction data of a ruby standard crystal ($Al_2O_3$) was refined using the above two values of $\alpha$ for the graphite (00.2) monochromator. The hexagonal unit cell of $Al_2O_3$ contains two molecular units (space group $R\bar{3}c$). The measurements were made at room temperature from the spherically shaped crystal of mean radius 0·16 mm, which was mounted on a Non-ius CAD4 automated diffractometer, and a full Cu $K\alpha$ sphere of data was collected ($\theta_{max} = 75°$). The data set included 576 reflections, and the integrated intensities were corrected for Lorentz factor, polarization and absorption using the spherical crystal model.

The effects of the incorrect $\alpha$ were first studied by using the complete data set in a simultaneous refinement of the positional parameters ($x, y, z$), thermal parameters $\beta_{ij}$, extinction parameter $\Gamma$ of the isotropic type I model of Becker & Coppens (1974) with a Lorentzian mosaic-spread distribution, and the scale factor $C$. The number of parameters to be refined is ten. The full-matrix least-squares refinements were based on $F_o^2$'s and weights $1/\sigma^2$, where $\sigma^2 =$

$\sigma_{count}^2 + (0\cdot04F_o^2)^2$. The reflections for which the extinction correction would have exceeded 20% were excluded from the refinement. The differences of the model parameters that arise from $\Delta\alpha = 1\cdot25-1\cdot10$ are given in Tables 2 and 3. The scale is lowered by 1·7%, which compensates the too small average value of $K_{pol}$, and the angle-dependent effects are absorbed by the extinction correction.

Further comparisons were made using terminated data sets, where sin $\theta/\lambda$ was limited to 0·55 and 0·5 Å⁻¹. In the latter case the extinction correction diverged, and therefore $\Gamma$ was fixed to the value obtained with sin $\theta/\lambda < 0\cdot55$ Å⁻¹. The effects of $\Delta\alpha$ become absorbed by the $\beta_{ij}$'s, as expected from the shape of the curves in Fig. 2. It can, however, be noted that the changes in the structural parameters obtained from data sets with different sin $\theta/\lambda$ termination are larger than the differences observed due to incorrect polarization correction of data sets of the same resolution. The thermal parameter $B$ defined as $8\pi^2(1/6)\sum U_{ii}$, for instance, increases by 0·276 Å² when the correctly treated data are terminated at sin $\theta/\lambda = 0\cdot55$ Å⁻¹ and by 0·600 Å² when they are terminated at 0·50 Å⁻¹.

The above findings demonstrate that the effects of an incorrect $\alpha$ can be complex. The fact that the fit is not improved when the correct $\alpha$ is used suggests that other errors in the models cause larger errors in the structural parameters. It is well known that the scattering factors based on spherical atomic electron distributions do not properly account for the bonding electrons especially in the low-angle reflections. In certain structures the use of a harmonic thermal model is not adequate. In this case additional problems may be caused by an incorrect angular behavior of the extinction correction. It is commonly observed that, in the case of large extinction, the strong reflections are overcorrected and these reflections cluster at small angles. When the data are limited to small scattering

angles the effect on the thermal parameters may be appreciable.

On some occasions the polarization ratio $K$ has been included in the parameters that are refined. The results have not been encouraging as the values may have fallen far outside the bounds of direct determinations (Vincent & Flack, 1980; Bachmann, Kohler, Schulz & Weber, 1984). This is not very surprising in the light of the above findings, which demonstrate that a smooth angular function can be absorbed in the model in many different ways.

The users of diffractometers are urged to determine $K$ experimentally, or at least to make an estimate as outlined in the *Introduction*. The values given in Table 1 suggest that the dynamical value for $K$ is a better estimate than the customarily used kinematical value. Jennings (1984) lists 40 determinations of $K$ in a survey conducted for the International Union of Crystallography Commission on Crystallographic Apparatus. These results also give guidelines for an estimation of $K$.

**References**

BACHMANN, R., KOHLER, H., SCHULZ, H. & WEBER, H.-P. (1984). *Acta Cryst.* A40, C400.
BECKER, P. J. & COPPENS, P. (1974). *Acta Cryst.* A30, 129–147.
JAMES, R. W. (1962). *The Optical Principles of the Diffraction of X-rays.* London: G. Bell and Sons.
JENNINGS, L. D. (1981). *Acta Cryst.* A37, 584–593.
JENNINGS, L. D. (1984). *Acta Cryst.* A40, 12–16.
LE PAGE, Y., GABE, E. J. & CALVERT, L. D. (1979). *J. Appl. Cryst.* 12, 25–26.
MATERLIK, G. & SUORTTI, P. (1984). *J. Appl. Cryst.* 17, 7–12.
OLEKHNOVICH, N. M. (1969). *Sov. Phys. Crystallogr.* 14, 203–206.
OLEKHNOVICH, N. M., MARKOVICH, V. L., OLEKHNOVICH, A. N. & POLUCHANKINA, L. P. (1981). *Izv. Akad. Nauk BSSR*, No. 2, 64–67.
SUORTTI, P. & JENNINGS, L. D. (1977). *Acta Cryst.* A33, 1012–1027.
VINCENT, M. G. & FLACK, H. D. (1980). *Acta Cryst.* A36, 614–620.
ZACHARIASEN, W. H. (1945). *Theory of X-ray Diffraction in Crystals.* New York: John Wiley & Sons.

---

# Neutron Diffraction from Single-Crystal Silicon: the Dependence of the Thermal Diffuse Scattering on the Velocity of Sound

BY B. T. M. WILLIS*

*AERE Harwell, Didcot, Oxon OX11 0RA, England*

AND C. J. CARLILE AND R. C. WARD

*Rutherford Appleton Laboratory, Chilton, Didcot, Oxon OX11 0QX, England*

## Abstract

It is well known [Willis (1970). *Acta Cryst.* A26, 396–401] from the theory of one-phonon scattering of thermal neutrons by a crystal that the nature of the thermal diffuse scattering (TDS) near the Bragg peak depends on whether the neutron velocity is greater than or is less than the sound velocity in the crystal. For faster-than-sound neutrons the TDS rises to a peak coinciding with the Bragg peak, whereas for slower-than-sound neutrons the TDS tends to give a flat background across the Bragg reflection. These theoretical predictions are supported by experiments using pulsed neutron diffraction from single crystals of perfect silicon. In particular, the integrated TDS across a reflection undergoes a pronounced fall when the neutron velocity drops below the velocity of sound.

---

* Now at: Chemical Crystallography Laboratory, 9 Parks Road, Oxford OX1 3PD, England.

## 1. Introduction

In a diffraction experiment, with either a single crystal or a polycrystalline sample, the measured intensity of a Bragg reflection will include a contribution from thermal diffuse scattering (TDS) which arises from the scattering of the incident beam by phonons. For X-rays, the one-phonon TDS is not subtracted with the background measured on either side of the reflection, since it rises to a maximum at the same point as the Bragg peak itself. This then causes the so-called TDS error in estimating Bragg intensities.

For thermal neutrons, the situation is quite different (Willis, 1970). The reason is that the neutron energy is comparable with the phonon energy, whereas X-rays have energies that are five orders of magnitude higher. Consequently, the condition

$$|\mathbf{k}| = |\mathbf{k}_0| \tag{1}$$

(where $\mathbf{k}$ and $\mathbf{k}_0$ are the wave vectors of the scattered